

Heterogeneous Contrastive Learning

Lecheng Zheng¹, Yada Zhu², Jingrui He¹ and Jinjun Xiong²

¹University of Illinois at Urbana-Champaign, {lecheng4, jingrui}@illinois.edu;

²IBM, {yzhu, jinjun}@us.ibm.com

ABSTRACT

With the advent of big data across multiple high-impact applications, we are often facing the challenge of complex heterogeneity. The newly collected data usually consist of multiple modalities, and characterized with multiple labels, thus exhibiting the co-existence of multiple types of heterogeneity. Although state-of-the-art techniques are good at modeling the complex heterogeneity with sufficient label information, such label information can be quite expensive to obtain in real applications, leading to sub-optimal performance using these techniques. Inspired by the capability of contrastive learning to utilize rich unlabeled data for improving performance, in this paper, we propose a unified heterogeneous learning framework, which combines both weighted unsupervised contrastive loss and weighted supervised contrastive loss to model multiple types of heterogeneity. We also provide theoretical analyses showing that the proposed weighted supervised contrastive loss is the lower bound of the mutual information of two samples from the same class and the weighted unsupervised contrastive loss is the lower bound of the mutual information between the hidden representation of two views of the same sample. Experimental results on real-world data sets demonstrate the effectiveness and the efficiency of the proposed method modeling multiple types of heterogeneity.

1 INTRODUCTION

Recent years have witnessed the surge of big data. According to a report published in Forbes*, the amount of newly created data in the past two years had increased by more than two trillion gigabytes. One major characteristic of big data is variety or heterogeneity. Furthermore, many high-impact applications exhibit complex heterogeneity or the co-existence of multiple types of data heterogeneity. For example, in social media, a post may consist of both image data and text data, i.e., view heterogeneity, and it can be assigned multiple tags based on the content, i.e., label heterogeneity; in the financial domain, the stock data may be collected from multiple sources (e.g., financial reports, weather, and news)[37], and the corresponding labels may not only include the stock price but also the price trend or volatility. To model such complex heterogeneity, heterogeneous learning has been studied for decades. Initial efforts focused on shallow machine learning algorithms modeling single heterogeneity (e.g., [11, 20, 34, 36, 38]), or dual heterogeneity (e.g., [7, 8, 16]). More recently, many researchers started exploring deep neural network based algorithms [15, 17, 18, 35], which achieved state-of-the-art performance in many scenarios. However, most (if not all) of these algorithms rely on a large amount of label information to build accurate models, which can be expensive and time-consuming to obtain in real applications. In other words, if applied on a data set consisting of a large amount of unlabeled data and only a small

percentage of labeled data, these algorithms may only lead to sub-optimal performance.

To address this limitation, in this paper, we propose a unified Heterogeneous Contrastive Learning framework, named *HCL*, which jointly models the view and label heterogeneity using two contrastive loss terms. In particular, to leverage a large amount of unlabeled data, we propose a weighted unsupervised contrastive loss, which automatically adjusts the weights of the samples drawn from the negative set based on the similarity of their original features; to leverage the limited labeled data, we propose a weighted supervised contrastive loss to group the samples with similar label vector together in the latent space, where the weights reflect how similar the label vectors of two samples are. By combining these two contrastive loss terms, our proposed framework is capable of modeling multiple types of heterogeneity in the presence of insufficient label information. In addition, we provide theoretical analysis to show that our proposed weighted unsupervised loss is the lower bound of the mutual information between the hidden representation of two views of the same sample and that the weighted supervised contrastive loss is the lower bound of the mutual information between two samples from the same class. Our main contributions are summarized below:

- A novel framework for deep heterogeneous contrastive learning, which effectively leverages a large amount of unlabeled data in the presence of limited labeled information.
- Theoretical analysis to show that the two weighted contrastive losses are the lower bound of the mutual information between two views of the same sample and the lower bound of the mutual information between two samples with similar label vector.
- Experimental results on real-world data sets, which demonstrate the effectiveness and the efficiency of the proposed model.

The rest of this paper is organized as follows. After a brief review of the related work in Section 2, we introduce our proposed model for heterogeneous contrastive learning in Section 3. The systematic evaluation of the proposed method on real-world data sets is presented in Section 4 before we conclude the paper in Section 5.

2 RELATED WORK

In this section, we briefly review the related work on contrastive learning and heterogeneous learning, specifically on multi-view learning, multi-label learning, and multi-class learning.

2.1 Contrastive Learning

Recently, contrastive learning attracts researchers' great attention due to its prominent performance for the unsupervised data. [26] is one of the earliest works, which proposes Contrastive Predictive Coding (CPC) framework to extract useful information from high dimensional data with a theoretical guarantee. Based on this work,

*<https://www.forbes.com/sites/gilpress/2020/01/06/6-predictions-about-data-in-2020-and-the-coming-decade/?sh=3214c68f4fc3>

recent studies [5, 6, 10, 24, 25] reveal a surge of research interest in contrastive learning. [25] extends CPC to a multi-view setting and learns a representation to maximize the mutual information between different views of the same sample. [6] proposes a debiased contrastive objective to reduce the weight of the samples that are similar to the positive samples. [24] proposes a novel estimator to jointly identify multiple positive samples and derives a tighter lower bound without additional computational costs. In [10], the authors extend CPC to the supervised scenario and consider the situation where the hidden representation of the samples from the same class should be close to each other in the latent space. [5] proposes a simple framework for contrastive learning of visual representations and boosts the performance of supervised and semi-supervised tasks on Image-Net. Although multi-view contrastive learning [25] is proposed to model the view-heterogeneity, it fails to consider the potential similarity of the hidden representations between the positive sample and the sample drawn from negative sets. Similarly, supervised contrastive loss (SupCon) [10] could not be directly applied to handle the multi-label scenario. Different from these works, in this paper, we propose both the weighted unsupervised contrastive loss and the weighted supervised contrastive loss to maximize the mutual information between the hidden representation of two views from the sample and the mutual information between the hidden representation of two samples from the same class.

2.2 Heterogeneous Learning

In this subsection, we mainly review the recent works on multi-view learning, multi-label learning, and multi-class learning. The initial works mainly focused on co-training [3], multiple kernel method [12], and subspace learning [1], multi-view learning has been studied for decades. More recently, more and more attention is paid to the direction of subspace learning. For example, [29] proposes a multi-view intact space learning method by integrating the encoded complementary information from multiple views to discover a latent representation; [30] assumes that different views are generated from the shared latent subspace and restored the incomplete view by exploiting the connection between multiple views; [19] performs semi-supervised classification and local structure learning simultaneously and automatically allocates weight for each view. In multi-label learning, [39] proposes a novel algorithm named "GLO-CAL", which exploits both global and local label correlations to learn a latent representation for both full-label and missing label scenarios. [31] tackles the extreme multi-label scenario and proposes a novel low-rank matrix decomposition method to handle the long tail problem with theoretical support. [21] presents one of the most popular feature estimation methods, namely "ReliefF" algorithm, to transform the multi-label problem into a single-label problem, and a distance function is defined to reduce the negative impact of the noisy features. [9] proposes "MIMLfast" approach by constructing a low-dimensional subspace shared by all labels, exploiting label relations within the shared subspace and optimizing the approximated ranking loss for the label-specific linear models via stochastic gradient descent. In multi-class learning, [23] proposes a novel metric learning objective function called multi-class N-pair loss, which allows joint comparison among N-1 negative examples and reduces the computational costs of computing deep embedding vectors. [32]

presents a semi-supervised multi-class active learning method by exploiting the active pool to evaluate the uncertainty of data and imposing a diversity constraint to select the diverse data and to reduce the uncertainty. In this paper, we propose the weighted unsupervised contrastive loss to maximize the mutual information between the hidden representation of two views and model the label correlation by maximizing the mutual information between the samples with the same label via weighted supervised contrastive loss.

3 PROPOSED HCL FRAMEWORK

In this section, we introduce our proposed framework for heterogeneous contrastive learning named *HCL*. We start by introducing the notation and then present the overall loss function with two regularization terms leveraging the labeled and unlabeled data respectively. Finally, we provide theoretical analysis regarding the two regularization terms.

3.1 Notation

Throughout this paper, we use lower-case letters for scalars (e.g., γ), and a bold upper-case letter for a matrix (e.g., X). We assume that the input data \mathcal{D} consists of two parts, namely $\mathcal{D} = \{\mathcal{L}, \mathcal{U}\}$. We use $\mathcal{L} = \{X^{\mathcal{L}}, Y^{\mathcal{L}}\}$ to denote the labeled data set, where $X^{\mathcal{L}} \in \mathbb{R}^{n \times d}$ and $Y^{\mathcal{L}} \in \mathbb{R}^{n \times c}$ are the input feature and binary label matrix for the labeled data set, respectively, n is the number of the labeled samples, d is the dimensionality of the input features, and c is the number of labels. $Y_i^{\mathcal{L}}(a)$ is the a^{th} binary label of sample $X_i^{\mathcal{L}}$. Similarly, we denote $\mathcal{U} = \{X^{\mathcal{U}}\}$ as the unlabeled data set, where $X^{\mathcal{U}} \in \mathbb{R}^{m \times d}$ is the input feature matrix for the unlabeled data set and m is the number of the unlabeled samples. Let $Z^{\mathcal{L}}$ be the hidden representation of labeled data generated by the encoder $E(\cdot)$, i.e., $Z^{\mathcal{L}} = E(X^{\mathcal{L}})$, and $Z^{\mathcal{U}}$ be the hidden representation of unlabeled data generated by the same encoder $E(\cdot)$, i.e., $Z^{\mathcal{U}} = E(X^{\mathcal{U}})$. For the ease of explanation, we denote X_i as a sample from either the labeled data set or the unlabeled data set when there is no confusion in a specific context and Z_i as the hidden representation of X_i .

Furthermore, in the presence of view heterogeneity, we assume that sample X_i is characterized by two views [†]: we denote $X_{i,1}$ and $X_{i,2}$ as the first and second views of X_i , respectively. For the two views, we could use two different encoders E_1 and E_2 to obtain the corresponding hidden representation $Z_{i,1}$ and $Z_{i,2}$, where $Z_{i,1} = E_1(X_{i,1})$ and $Z_{i,2} = E_2(X_{i,2})$ are the representation extracted from the first view and the second view, respectively.

3.2 Objective Function

Now, we are ready to introduce the overall objective function:

$$\begin{aligned} \min J = & L_c(Y^{\mathcal{L}}, \hat{Y}^{\mathcal{L}}) + \alpha L_u(X^{\mathcal{L}}, X^{\mathcal{U}}, Z^{\mathcal{L}}, Z^{\mathcal{U}}) \\ & + \beta L_s(Z^{\mathcal{L}}, Y^{\mathcal{L}}) \end{aligned} \quad (1)$$

where $\hat{Y}^{\mathcal{L}}$ is the prediction made by the classifier $C(\cdot)$, i.e., $\hat{Y}^{\mathcal{L}} = C(Z^{\mathcal{L}})$, L_c is the cross entropy loss, L_u is the unsupervised contrastive loss to model multi-view heterogeneity by regularizing the hidden feature representation $Z^{\mathcal{L}}$, and $Z^{\mathcal{U}}$, L_s is the supervised contrastive loss to model multi-label or multi-class heterogeneity

[†]If only one view is available, we could use two different data augmentation methods to generate two views by following the strategy mentioned in [5].

by regularizing the hidden feature representation $Z^{\mathcal{L}}$, and α and β are two positive hyper-parameters balancing the two regularization terms. Next, we elaborate on each regularization term respectively.

3.2.1 L_u : Weighted Unsupervised Contrastive Loss. The main idea of the unsupervised contrastive loss is to utilize the rich unlabeled data to enhance the quality of the hidden representation. Following [24], it can be written as follows:

$$L = -\mathbb{E}_{X_i \in \mathcal{D}} [\log \frac{f(X_i, Z_i)}{f(X_i, Z_i) + \sum_{k \neq i} f(X_i, Z_k)}] \quad (2)$$

where $f(\cdot, \cdot)$ is the similarity measurement function, e.g., $f(a, b) = \exp(\frac{a \cdot b}{\tau})$, τ is the temperature, and X_i is a sample drawn from \mathcal{D} . Following [24], (X_i, Z_i) in the numerator is considered as a positive pair and (X_i, Z_k) in the denominator is considered as a negative pair. Eq. 2 aims to maximize the mutual information between the original input features and the hidden representations by minimizing the unsupervised contrastive learning loss. Though this unsupervised contrastive loss takes advantage of the rich information from the unlabeled data, it does not take into consideration the case where two samples with similar input features tend to have similar hidden representation.

To address this issue, we propose the weighted unsupervised contrastive learning loss, which fully considers the potential similarity of the hidden representation of the negative pair by re-weighting all negative pairs. For the ease of explanation, we denote the negative set as $\mathcal{N}_i^{\mathcal{D}} = \mathcal{D} \setminus \{i\}$, which consists of the entire data set except for X_i . The weighted unsupervised contrastive learning loss can be formulated as follows:

$$L_u = -\mathbb{E}_{X_i \in \mathcal{D}} [\log \frac{f(X_i, Z_i)}{f(X_i, Z_i) + \sum_{X_k \in \mathcal{N}_i^{\mathcal{D}}} g(X_i, X_k) f(X_i, Z_k)}] \quad (3)$$

where $g(X_i, X_k)$ is a similarity measurement between X_i and X_k , e.g. $g(X_i, X_k) = \exp(1 - \frac{|X_i - X_k|}{|X_i| |X_k|})$. The intuition of $g(X_i, X_k)$ is that if two samples chosen as a negative pair are similar in terms of the input feature similarity, they are very likely to have the similar hidden representations. Thus, we reduce the weight of this negative pair based on how similar their original features are.

The proposed weighted unsupervised contrastive loss can be naturally extended to model multi-view data. Different from the intuition of contrastive learning for a single view, the multi-view contrastive loss aims to maximize the mutual information of the hidden representation of two views. More specifically, given a sample X_i with two views $X_{i,1}$ and $X_{i,2}$, the weighted unsupervised contrastive loss could be updated as follows:

$$L_u = -\mathbb{E}_{X_i \in \mathcal{D}} [\log \frac{f(Z_{i,1}, Z_{i,2})}{f(Z_{i,1}, Z_{i,2}) + \sum_{X_k \in \mathcal{N}_i^{\mathcal{D}}} g(X_{i,1}, X_{k,j}) f(Z_{i,1}, Z_{k,j})}] \quad (4)$$

where we denote $X_{k,j}$ to be the j^{th} view of X_k , $Z_{k,j}$ is the hidden representation of $X_{k,j}$ and $\mathcal{N}_i^{\mathcal{D}} = \mathcal{D} \setminus \{i\}$. This equation aims to maximize the mutual information between the hidden representation extracted from two views and to minimize the similarity of the hidden representation extracted from two different samples. Notice that in the denominator of this equation, we follow [5] to include

| - | Noisy MNIST | CelebA |
|--------------------------------|-------------|-------------|
| Setting | Multi-class | Multi-label |
| Number of labels | 10 | 40 |
| Size of data set | 70,000 | 202,599 |
| Number of unique label vectors | 10 | 115,114 |
| Average size of positive set | 7,000 | 1.76 |
| Largest size of positive set | 7877 | 358 |

Table 1: Statistics of label information for two data sets

both the first view and the second view of X_k as the negative samples in order to increase the size of the negative set. As the size of the negative set increases, we tend to have a tighter lower bound, which is demonstrated in Lemma 3.2 and Section 4.5 Parameter analysis. The extension to more than two views is straightforward [‡], and we omit it for brevity.

3.2.2 L_s : Weighted Supervised Contrastive Loss. The goal of the supervised contrastive loss is to maximize the mutual information between two samples with the same label [10]. In the binary classification setting ($c = 1$), we denote the set of positive samples drawn from the labeled data set as $\mathcal{P}^{\mathcal{L}} = \{X_j | Y_j^{\mathcal{L}} = 1\}$ and the set of the negative samples drawn from the labeled data set as $\mathcal{N}^{\mathcal{L}} = \{X_k | Y_k^{\mathcal{L}} \neq 1\}$. Based on [10], the supervised contrastive learning loss (SupCon) is formulated as follows:

$$L_{\text{sup}} = -\mathbb{E}_{X_i, X_j \in \mathcal{P}^{\mathcal{L}}} [\log \frac{f(S_i, S_j)}{f(S_i, S_j) + \sum_{X_k \in \mathcal{N}^{\mathcal{L}}} f(S_i, S_k)}] \quad (5)$$

where $S_i = \text{concat}(Z_{i,1}, Z_{i,2})$ is the concatenation of the hidden representation for the two views of X_i ($S_i = Z_{i,1}$ if only one view is available). The intuition of this equation is that any pair of samples drawn from the positive set $\mathcal{P}^{\mathcal{L}}$ should be closer than the samples from the negative set $\mathcal{N}^{\mathcal{L}}$ in the latent space. Despite its superior performance, SupCon is not designed for the multi-label setting. Different from the binary classification problem or multi-class problem where a sample could only be classified into one class, in the multi-label setting, a sample could be characterized with multiple labels. As the number of the labels c increases, it becomes harder to find two samples with the same label vector (as there are 2^c different combinations for c different binary labels). For example, Table 1 shows the statistics of label information for the Noisy MNIST data set [27] and the CelebA data set [14]. By observation, we could see that in the multi-label setting, there are 115,114 unique label vectors in the CelebA data set, and the average size of the positive set is only 1.76, which is largely different from that for the Noisy MNIST data set in the multi-class setting. This indicates that SupCon is not applicable in the multi-label setting as it is impossible to construct the positive set that contains at least two samples for each unique label vector for contrastive learning.

To overcome this issue, we propose the weighted supervised contrastive loss formulated as follows:

$$L_s = -\frac{1}{c} \sum_{a=1}^c \mathbb{E}_{X_i, X_j \in \mathcal{P}^{\mathcal{L}}(a)} [\log \frac{\sigma f(S_i, S_j)}{\sigma f(S_i, S_j) + \sum_{X_k \in \mathcal{N}^{\mathcal{L}}(a)} \gamma f(S_i, S_k)}] \quad (6)$$

$$\sigma = 1 - \text{dist}(Y_i^{\mathcal{L}}, Y_j^{\mathcal{L}})/c, \gamma = \text{dist}(Y_i^{\mathcal{L}}, Y_k^{\mathcal{L}})$$

[‡]We could maximize the sum of the mutual information between any pairs of two views.

where $dist(Y_i^{\mathcal{L}}, Y_k^{\mathcal{L}})$ is the distance measurement between two label vectors, e.g., hamming distance, $\mathcal{P}^{\mathcal{L}}(a) = \{X_j | Y_j^{\mathcal{L}}(a) = 1\}$ is the set of positive samples drawn from the labeled data set in terms of the a^{th} label and $\mathcal{N}^{\mathcal{L}}(a) = \{X_k | Y_k^{\mathcal{L}}(a) \neq 1\}$ is the set of the negative samples. The intuition of Eq. 6 is that the samples with similar label vectors should be close to each other in the latent space, and the magnitude of the similarity is determined based on how similar their label vectors are. Specifically, in the numerator of Eq. 6, we aim to maximize the similarity between the hidden representation of X_i and X_j if the a^{th} binary labels for these two samples are both positive, i.e., $Y_i^{\mathcal{L}}(a) = Y_j^{\mathcal{L}}(a) = 1$. However, in the multi-label setting, since one sample could be characterized by multiple labels, we reweight the similarity of the hidden representation by the function σ such that if the label vectors of the two samples are identical, σ is equal to 1, and it gradually approaches to 0 as the two label vectors become completely different. Similarly, in the denominator, we aim to minimize the similarity between the hidden representation of samples X_i and X_k if their a^{th} labels are different and the similarity measurement is also weighted based on how dissimilar their label vectors are.

3.3 Special Cases

The existing contrastive losses proposed in SupCon [10] and SimCLR [5] can be considered as special cases of our proposed framework. First of all, the weighted supervised contrastive loss in our proposed method can be degraded to SupCon. In the binary classification setting or multi-class setting, the distance measurement function $dist(Y_i^{\mathcal{L}}, Y_j^{\mathcal{L}})$ in Eq. 6 can be reduced to an indicator function $dist(Y_i^{\mathcal{L}}, Y_j^{\mathcal{L}}) = 1_{Y_i^{\mathcal{L}} \neq Y_j^{\mathcal{L}}}$, where $1_{Y_i^{\mathcal{L}} \neq Y_j^{\mathcal{L}}} = 0$ if $Y_i^{\mathcal{L}} = Y_j^{\mathcal{L}}$ and $1_{Y_i^{\mathcal{L}} \neq Y_j^{\mathcal{L}}} = 1$ otherwise (as $Y_i^{\mathcal{L}}$ and $Y_j^{\mathcal{L}}$ are scalars in the binary classification setting or multi-class setting). In this case, the weight imposed on the positive pair in the numerator of Eq. 6 is reduced to $\sigma = 1 - dist(Y_i^{\mathcal{L}}, Y_j^{\mathcal{L}})/c = 1 - 1_{Y_i^{\mathcal{L}} \neq Y_j^{\mathcal{L}}} = 1$ because $Y_i^{\mathcal{L}} = Y_j^{\mathcal{L}}$ for any positive pairs. Similarly, the weight $dist(Y_i^{\mathcal{L}}, Y_k^{\mathcal{L}}) = 1_{Y_i^{\mathcal{L}} \neq Y_k^{\mathcal{L}}}$ imposed on the denominator is equal to 1 because $Y_i^{\mathcal{L}} \neq Y_k^{\mathcal{L}}$ for any negative pairs. Thus, in the binary classification or multi-class setting, Eq. 6 could be reduced to Eq. 5, which is exactly the formulation of SupCon. Compared with SupCon, our proposed method can not only handle the multi-class problem but also the multi-label classification problem.

Similarly, the weighted unsupervised contrastive loss in our proposed method can also be degraded to the objective function in SimCLR by setting the weights of all negative pairs to 1.

3.4 Theoretical Analysis

In this subsection, we provide the analysis regarding the properties of the two proposed contrastive losses.

LEMMA 3.1. *Given two samples X_i and X_j from the same class, e.g., $Y_i(a) = Y_j(a) = 1$, drawn from the labeled set \mathcal{L} , we have $I(X_i, X_j) \geq -\frac{1}{\epsilon}(L_s - N)$, where $I(X_i, X_j)$ is the mutual information between X_i and X_j , L_s is the supervised contrastive loss weighted by hamming distance measurement, ϵ is the number of*

times when the binary labels of two samples X_i and X_j are positive, e.g., $Y_i(a) = Y_j(a) = 1, a = 1, \dots, c$, and $N = \frac{1}{c} \sum_{a=1}^c \log(|\mathcal{N}^{\mathcal{L}}(a)|)$.

Proof: *Following the theoretical analysis in [26], the optimal value of $f(S_i, S_j)$ is given by $\frac{P(X_j|X_i)}{P(X_j)}$. Thus, the weighted supervised contrastive loss could be rewritten as follows:*

$$\begin{aligned} L_s &= -\frac{1}{c} \sum_{a=1}^c \mathbb{E}_{X_i, X_j \in \mathcal{P}^{\mathcal{L}}(a)} [\log \frac{\sigma f(S_i, S_j)}{\sigma f(S_i, S_j) + \sum_{X_k \in \mathcal{N}^{\mathcal{L}}(a)} \gamma f(S_i, S_k)}] \\ &= \frac{1}{c} \sum_{a=1}^c \mathbb{E}_{X_i, X_j \in \mathcal{P}^{\mathcal{L}}(a)} [\log \frac{\sigma f(S_i, S_j) + \sum_{X_k \in \mathcal{N}^{\mathcal{L}}(a)} \gamma f(S_i, S_k)}{\sigma f(S_i, S_j)}] \\ &= \frac{1}{c} \sum_{a=1}^c \mathbb{E}_{X_i, X_j \in \mathcal{P}^{\mathcal{L}}(a)} [\log \frac{\sigma \frac{P(X_j|X_i)}{P(X_j)} + \sum_{X_k \in \mathcal{N}^{\mathcal{L}}(a)} \gamma \frac{P(X_k|X_i)}{P(X_k)}}{\sigma \frac{P(X_j|X_i)}{P(X_j)}}] \\ &= \frac{1}{c} \sum_{a=1}^c \mathbb{E}_{X_i, X_j \in \mathcal{P}^{\mathcal{L}}(a)} [\log(1 + \frac{P(X_j)}{\sigma P(X_j|X_i)} \sum_{X_k \in \mathcal{N}^{\mathcal{L}}(a)} \gamma \frac{P(X_k|X_i)}{P(X_k)})] \end{aligned}$$

Since $(X_i^{\mathcal{L}}, X_k^{\mathcal{L}})$ is defined as a negative pair, it means that at least one binary label does not match for this negative pair. Therefore, we have $\gamma = dist(Y_i^{\mathcal{L}}, Y_k^{\mathcal{L}}) \in [1, c]$ for all negative pairs and $\sigma \in [\frac{1}{c}, 1]$ for all positive pairs with hamming distance measurement, which leads to $\frac{P(X_j)}{\sigma P(X_j|X_i)} \geq \frac{P(X_j)}{P(X_j|X_i)}$ and $\gamma \frac{P(X_k|X_i)}{P(X_k)} \geq \frac{P(X_k|X_i)}{P(X_k)}$. Thus, we have

$$\begin{aligned} L_s &\geq \frac{1}{c} \sum_{a=1}^c \mathbb{E}_{X_i, X_j \in \mathcal{P}^{\mathcal{L}}(a)} [\log(1 + \frac{P(X_j)}{P(X_j|X_i)} \sum_{X_k \in \mathcal{N}^{\mathcal{L}}(a)} \frac{P(X_k|X_i)}{P(X_k)})] \\ &\approx \frac{1}{c} \sum_{a=1}^c \mathbb{E}_{X_i, X_j \in \mathcal{P}^{\mathcal{L}}(a)} [\log(1 + \frac{P(X_j)}{P(X_j|X_i)} (|\mathcal{N}^{\mathcal{L}}(a)| \mathbb{E}_{X_k} \frac{P(X_k|X_i)}{P(X_k)}))] \\ &= \frac{1}{c} \sum_{a=1}^c \mathbb{E}_{X_i, X_j \in \mathcal{P}^{\mathcal{L}}(a)} [\log(1 + \frac{P(X_j)}{P(X_j|X_i)} |\mathcal{N}^{\mathcal{L}}(a)|)] \\ &\geq \frac{1}{c} \sum_{a=1}^c \mathbb{E}_{X_i, X_j \in \mathcal{P}^{\mathcal{L}}(a)} [\log(\frac{P(X_j)}{P(X_j|X_i)}) + \log(|\mathcal{N}^{\mathcal{L}}(a)|)] \\ &= -\frac{1}{c} \sum_{a=1}^c I(X_i, X_j) + \frac{1}{c} \sum_{a=1}^c \log(|\mathcal{N}^{\mathcal{L}}(a)|) \\ &= -\epsilon I(X_i, X_j) + N \end{aligned}$$

where $|\mathcal{N}^{\mathcal{L}}(a)|$ is the number of negative pairs for the a^{th} label, $N = \frac{1}{c} \sum_{a=1}^c \log(|\mathcal{N}^{\mathcal{L}}(a)|)$ and ϵ is the number of times when the binary labels of two samples X_i and X_j are positive, e.g., $Y_i(a) = Y_j(a) = 1, a = 1, \dots, c$. Finally, we have $I(X_i, X_j) \geq -\frac{1}{\epsilon}(L_s - N)$, which completes the proof.

LEMMA 3.2. *Given a sample X_i drawn from the entire set \mathcal{D} , we have $I(X_{i,1}, X_{i,2}) \geq -L_u + \log(|\mathcal{N}_i^{\mathcal{D}}|)$, where $I(X_{i,1}, X_{i,2})$ is the mutual information between $X_{i,1}$ and $X_{i,2}$, L_u is the unsupervised contrastive loss weighted by $g(X_i, X_k) = \exp(1 - \frac{X_i \cdot X_k}{|X_i| |X_k|})$ and $|\mathcal{N}_i^{\mathcal{D}}|$ is the size of negative set.*

Proof: *Similar to the theoretical analysis in Lemma 3.1, the optimal value of $f(X_{i,1}, X_{i,2})$ is given by $\frac{P(X_{i,2}|X_{i,1})}{P(X_{i,2})}$. Thus, the*

weighted unsupervised contrastive loss could be rewritten as follows:

$$\begin{aligned} L_u &= -\mathbb{E}_{X_i \in \mathcal{D}} [\log \frac{f(Z_{i,1}, Z_{i,2})}{f(Z_{i,1}, Z_{i,2}) + \sum_{X_k \in \mathcal{N}_i^{\mathcal{D}}} g(X_{i,1}, X_{k,j}) f(Z_{i,1}, Z_{k,j})}] \\ &= \mathbb{E}_{X_i \in \mathcal{D}} [\log (1 + \frac{P(X_{i,2})}{P(X_{i,2}|X_{i,1})} \sum_{X_k \in \mathcal{N}_i^{\mathcal{D}}} \frac{g(X_{i,1}, X_{k,j}) P(X_{k,j}|X_{i,1})}{P(X_{k,j})})] \end{aligned}$$

Notice that $g(X_{i,1}, X_{k,j}) \in [1, e^2]$, so $g(X_{i,1}, X_{k,j}) \frac{P(X_{k,j}|X_{i,1})}{P(X_{k,j})} \geq \frac{P(X_{k,j}|X_{i,1})}{P(X_{k,j})}$. Similarly, we have

$$\begin{aligned} L_u &\geq \mathbb{E}_{X_i \in \mathcal{D}} [\log (1 + \frac{P(X_{i,2})}{P(X_{i,2}|X_{i,1})} \sum_{X_k \in \mathcal{N}_i^{\mathcal{D}}} \frac{P(X_{k,j}|X_{i,1})}{P(X_{k,j})})] \\ &\approx \mathbb{E}_{X_i \in \mathcal{D}} [\log (1 + \frac{P(X_{i,2})}{P(X_{i,2}|X_{i,1})} |\mathcal{N}_i^{\mathcal{D}}| \mathbb{E}_{X_k \in \mathcal{N}_i^{\mathcal{D}}} \frac{P(X_{k,j}|X_{i,1})}{P(X_{k,j})})] \\ &= \mathbb{E}_{X_i \in \mathcal{D}} [\log (1 + \frac{P(X_{i,2})}{P(X_{i,2}|X_{i,1})} |\mathcal{N}_i^{\mathcal{D}}|)] \\ &\geq \mathbb{E}_{X_i \in \mathcal{D}} [\log (\frac{P(X_{i,2})}{P(X_{i,2}|X_{i,1})}) + \log (|\mathcal{N}_i^{\mathcal{D}}|)] \\ &\geq -I(X_{i,1}, X_{i,2}) + \log (|\mathcal{N}_i^{\mathcal{D}}|) \end{aligned}$$

Finally, we have $I(X_{i,1}, X_{i,2}) \geq -L_u + \log (|\mathcal{N}_i^{\mathcal{D}}|)$, which completes the proof.

Based on the Lemma 3.1, we observe that the proposed weighted supervised contrastive loss is the lower bound of the mutual information of two samples from the class a . In Lemma 3.2, we prove that the weighted unsupervised contrastive loss is the lower bound of the mutual information between the hidden representation of two views of the same sample. As the size of the data set becomes larger, the lower bound becomes tighter, which is further demonstrated in Section 4.5 parameter analysis. Combining both weighted supervised contrastive loss and weighted unsupervised contrastive loss, we aim to explore the hidden representation that enjoys the following benefits: (1) if two samples are from the same class, then their hidden representations should be close to each other in the embedding space by minimizing L_s ; (2) the hidden representations should only contain the information shared by the two views and discard the irrelevant information as much as possible by minimizing L_u .

4 EXPERIMENTAL RESULTS

In this section, we demonstrate the performance of our proposed framework in terms of the effectiveness by comparing it with state-of-the-art methods. In addition, we conduct a case study to show how different levels of noise influence our proposed methods, which is followed by the parameter analysis and efficiency analysis.

4.1 Experiment Setup

Data Sets: We mainly evaluate our proposed algorithm on the following data sets: Noisy MNIST (N-MNIST)[§]; X-ray Microbeam

[§]<http://yann.lecun.com/exdb/mnist/>

(XRMB)[¶], Celebrity Face Attributes (CelebA)^{||} and Scene^{**}. N-MNIST [2] data set consists of 70,000 images of handwritten digits with an additive white gaussian noise added to the MNIST data set. Specifically, we add Gaussian noise to MNIST [13] data set to generate the N-MNIST data set by following the strategy introduced in [27]. We first rescale the pixel values of each image to [0,1], then add the random noise uniformly sample from [0, 1] to each pixel and finally truncate the pixel values to [0, 1]. Scene [4] is a single-view multi-label dataset characterized with six binary labels, which consists of 2,407 samples. XRMB [28] is a multi-view multi-class data set, which consists of 40 binary labels and two views. The first view is acoustic data with 273 features and the second view is articulatory data with 112 features. CelebA [14] is a large-scale face attributes dataset with more than 200K celebrity images, labeled with 40 attribute annotations. Following the strategy used in [5], we use two data augmentation methods, e.g., (1) crop and resize and (2) color distortion, to generate two views for the CelebA data set.

Experiment Setting The neural network structure and two hyper-parameters α and β for each data set are specified with the experimental results analysis. For each data set, we randomly draw the same amount of training samples, repeat the experiments five times, and report the mean and the standard deviation of F1 score and AUC metric. In all experiments, we set the initial learning rate to be 0.05 and the optimizer is momentum stochastic gradient descent with Layer-wise Adaptive Rate Scaling scheduler (LARS) [33]. Besides, we consider the test set as the unlabeled set \mathcal{U} , the similarity function $f(a, b)$ is defined as $f(a, b) = \exp(\frac{a \cdot b}{|a||b|})$ and $dist(Y_i^{\mathcal{L}}, Y_k^{\mathcal{L}})$ is the hamming distance measurement.

Reproducibility: All of the real-world data sets are publicly available. The code of our algorithms could be found in an anonymous link ^{††}. The experiments are performed on a Windows machine with a 16GB RTX 5000 GPU.

Comparison Methods: In our experiments, we compare our proposed method, i.e., *HCL* with following methods:

- DNN: a simple deep neural network, the structure of which will be specified for each data set;
- SimCLR [5]: a simple contrastive learning framework for image classification tasks in two views setting;
- CPC [26]: a contrastive learning method for self supervised learning in the single view setting;
- SupCon [10]: a supervised contrastive learning method in the single view setting;
- DeepMTMV [35]: a deep framework modeling both view heterogeneity and label heterogeneity;
- *HCL-u*: one variant of our proposed method by discarding the weighted supervised contrastive loss term;
- *HCL-s*: the second variant of our proposed method by discarding the weighted unsupervised contrastive loss term.

The neural network architecture of SimCLR, CPC, SupCon and our methods will be specified for each data set in different experimental settings. As some proposed methods are only designed for

[¶]https://ttic.uchicago.edu/~klivescu/XRMB_data/full/README

^{||}<http://mmlab.ie.cuhk.edu.hk/projects/CelebA.html>

^{**}<http://mulan.sourceforge.net/datasets-mlc.html>

^{††}<https://drive.google.com/file/d/1IKO0b42fWpUMHwsPADTMGLHDTzEJKJ17/view?usp=sharing>

| Model | Scene | | N-MNIST | |
|---------------|---------------------------------------|---------------------------------------|---------------------------------------|---------------------------------------|
| | F1 Score | AUC | F1 Score | AUC |
| DNN | 0.6056 \pm 0.0090 | 0.7819 \pm 0.0049 | 0.9018 \pm 0.0068 | 0.9454 \pm 0.0038 |
| CPC | 0.6265 \pm 0.0197 | 0.7979 \pm 0.0142 | 0.8852 \pm 0.0087 | 0.8860 \pm 0.0084 |
| DeepMTMV | 0.6173 \pm 0.0200 | 0.7991 \pm 0.0163 | 0.9045 \pm 0.0049 | 0.9472 \pm 0.0026 |
| SupCon | 0.6223 \pm 0.0233 | 0.8013 \pm 0.0178 | 0.9283 \pm 0.0025 | 0.9601 \pm 0.0014 |
| <i>HCL</i> -s | 0.6264 \pm 0.0190 | 0.8067 \pm 0.0140 | 0.9283 \pm 0.0025 | 0.9601 \pm 0.0014 |
| <i>HCL</i> -u | 0.6401 \pm 0.0181 | 0.8150 \pm 0.0134 | 0.9049 \pm 0.0030 | 0.9475 \pm 0.0016 |
| <i>HCL</i> | 0.6413 \pm 0.0193 | 0.8205 \pm 0.0121 | 0.9246 \pm 0.0028 | 0.9582 \pm 0.0016 |

Table 2: Results on Scene and N-MNIST data sets

a particular setting, (e.g., SimCLR for two views), we only report the performance of these baselines if applicable. In addition, for SimCLR algorithm, we change the neural network structure from convolutional layer to fully-connected layer to deal with non-image data. For data sets in multi-view setting, we concatenate the hidden representations for SupCon.

4.2 Single-view Multi-label Setting

In this subsection, we test the performance of our proposed method on two real-world data sets in the single-view multi-label setting, including Scene data set and N-MNIST data set. In the experiments, we use Eq. 3 to compute the weighted unsupervised contrastive loss for *HCL* and *HCL*-u.

For the Scene data set, we randomly sample 5% data (120 samples) as the training set and the rest 95% data as the test set. The number of binary labels is 6. The neural network architectures of DNN, CPC, SupCon, and our methods are the same, which is a three-layer fully-connected neural network. Two hyper-parameters α and β for *HCL* are 0.2 and 0.01, respectively, the hyper-parameter α for *HCL*-u is 0.3 and the hyper-parameter β for *HCL*-s is 0.01. The batch size is the entire training set, the number of epochs for our methods is 200 and the size of the negative set $|\mathcal{N}_i|$ is equal to 2,406 ($|\mathcal{D}| - 1$). Table 2 shows the performance of our proposed methods and state-of-the-art methods. By observation, we find that our proposed method *HCL* and *HCL*-u outperform all baseline models. Specifically, compared with CPC, *HCL*-u and *HCL* further boost the performance by 1.4% and 1.5% in terms of F1 score, respectively. This suggests that CPC indeed leads to sub-optimal performance as it assigns the same weight to each negative sample no matter how similar this negative sample is to the positive sample. From this table, we also observe that the performance of DeepMTMV is only better than DNN and worse than the rest methods. Our guess is that DeepMTMV suffers a lot from insufficient label information.

For the N-MNIST data set, we sampled 20 images for each digit from 10,000 images as our training set and the rest 60,000 samples are considered as our test set. The neural network architectures of DNN, CPC, SupCon, and our methods are the same, which is a two-layer convolutional layer followed by a max-pooling layer and a two-layer fully-connected neural network. Two hyper-parameters α and β for *HCL* are 0.001 and 6, respectively, the hyper-parameter α for *HCL*-u is 0.001 and the hyper-parameter β for *HCL*-s is 7. The batch size is 200 (the size of the entire labeled set), the number of iterations for our methods is 500 and the size of the negative set $|\mathcal{N}_i|$ is 4,199 (200 labeled samples and 4000 unlabeled samples for each

iteration). Based on Table 2, we observe that *HCL*-s and SupCon achieve the best F1 score and AUC (as we mentioned in Section 3.3, in multi-class setting, *HCL*-s could degrade to SupCon and thus their performance are the same). Different from the performance improvement in the Scene data set for unsupervised contrastive learning methods, in the N-MNIST data set, CPC and *HCL*-u fail to boost the predictive performance by leveraging unlabeled data. Instead, the performance of CPC becomes even worse than DNN and our guess is that the unsupervised contrastive loss term introduces noise into the hidden representation due to the added Gaussian noise. We further analyze how different noise levels influence both the unsupervised contrastive loss and supervised contrastive loss in a case study presented in Section 4.4.

4.3 Multi-view Multi-label Setting

In this subsection, we test the performance of our proposed method on two real-world data sets in a multi-view multi-label setting, including the XRMB data set and CelebA data set. In the experiments, we use Eq. 4 to compute the weighted unsupervised contrastive loss for *HCL* and *HCL*-u.

For the XRMB data set, we select the first 20 classes as the label and randomly draw 2,500 samples for each class (50,000 samples in total). We sample 250 data points as our training set and the rest 49,750 samples as our test set. The neural network architectures of DNN, SimCLR, SupCon, and our methods are the same, which is a three-layer fully-connected neural network. Two hyper-parameters α and β for *HCL* are 0.1 and 0.001, respectively, the hyper-parameter α for *HCL*-u is 0.1 and the hyper-parameter β for *HCL*-s is 0.0075. The batch size is 250, the number of epochs for our methods is 500 and the size of negative set $|\mathcal{N}_i|$ is equal to 4,999. Table 3 shows the performance of our proposed methods and state-of-the-art models. By observation, our proposed methods outperform all baselines in terms of F1 score and AUC. Similar to the observation in the Scene data set, DeepMTMV only achieves better performance than DNN and behaves worse than all contrastive learning based methods. Compared with SimCLR and SupCon, *HCL* boosts the performance by 2.2% and 1.8% in terms of F1 score, respectively.

For the CelebA data set, we randomly draw 500 samples as our training set and 49,500 samples as our test set. The number of binary labels is 40 and 9 out of 40 are labeled as positive on average. The neural network architectures of DNN, SimCLR, SupCon, and our methods are the same, which is a truncated version of vgg-13 [22], consisting of six convolutional layers, three max-pooling layers, and a three-layer fully-connected neural network. We set

| - | XRMB | | CelebA | |
|---------------|---------------------------------------|---------------------------------------|---------------------------------------|---------------------------------------|
| Model | F1 Score | AUC | F1 Score | AUC |
| DNN | 0.5492 ± 0.0100 | 0.7628 ± 0.0057 | 0.5453 ± 0.0092 | 0.5881 ± 0.0128 |
| SimCLR | 0.5594 ± 0.0214 | 0.7715 ± 0.0108 | 0.5563 ± 0.0151 | 0.5949 ± 0.0157 |
| DeepMTMV | 0.5570 ± 0.0152 | 0.7699 ± 0.0077 | 0.5559 ± 0.0124 | 0.5946 ± 0.0115 |
| SupCon | 0.5636 ± 0.0118 | 0.7737 ± 0.0063 | 0.5528 ± 0.0176 | 0.5920 ± 0.0173 |
| <i>HCL</i> -s | 0.5636 ± 0.0118 | 0.7737 ± 0.0063 | 0.5816 ± 0.0185 | 0.6217 ± 0.0177 |
| <i>HCL</i> -u | 0.5698 ± 0.0109 | 0.7727 ± 0.0066 | 0.5620 ± 0.0159 | 0.5976 ± 0.0154 |
| <i>HCL</i> | 0.5813 ± 0.0152 | 0.7825 ± 0.0094 | 0.5833 ± 0.0164 | 0.6226 ± 0.0173 |

Table 3: Results on XRMB and CelebA data sets

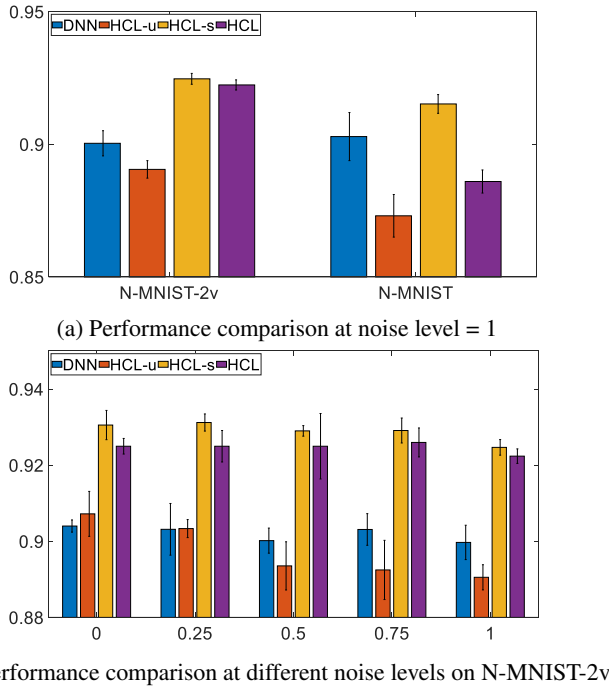


Figure 1: Performance comparison on N-MNIST data set with different level of noise in terms of F1 score (Best viewed in color)

two hyper-parameters $\alpha = 0.1$ and $\beta = 0.005$ for *HCL*, the hyper-parameter $\alpha = 0.1$ for *HCL*-u and the hyper-parameter $\beta = 0.0075$ for *HCL*-s. The batch size is 50, the number of epochs is 600 and the size of negative set $|\mathcal{N}_i|$ is 249. Table 3 shows the performance of our proposed methods and state-of-the-art baseline models. By observation, we could find that our proposed methods outperform all baselines in terms of both F1 score and AUC; DeepMTMV has better predictive results than both DNN and SupCon. As we mentioned in Section 3.2.2, due to a large number of unique label vectors in the CelebA data set, SupCon fails to maximize the similarity between the hidden representation of two samples with similar label vectors. Thus, Table 3 shows that SupCon only performs slightly better than DNN but is worse than the rest of the algorithms. Compared with SupCon, *HCL*-s and *HCL* improve the performance by 2.9% and 3.1% in terms of F1 score, respectively.

4.4 Case Study

In this subsection, we study how different noise level influences two weighted unsupervised contrastive loss term (i.e., Eq. 3 and Eq. 4) and weighted supervised contrastive loss term. We denote the single view Noisy MNIST as N-MNIST and two-view Noisy MNIST as N-MNIST-2v. For a fair comparison, our data preprocessing consists of the following steps: (1). we generate the noise matrix $\mathcal{N}(\mu, \sigma)$ with the same shape as the entire data set, where μ and σ are the mean and the standard deviation of the MNIST data set; (2). to generate different levels of noise, we sample different percentage of indices from the same noise matrix $\mathcal{N}(\mu, \sigma)$ (e.g., 0%, 25%, 50%, 75% and 100%) ^{††} and add them to the original MNIST data to generate N-MNIST, which is also considered as the first view of Noisy-MNIST-2v; (3). to generate the second view for N-MNIST-2v, we repeat step 2 to generate the second noise matrix $\mathcal{N}_2(\mu, \sigma)$ in order to create the second view. In this case study, we set the number of epochs for our methods to be 500, the batch size to be 200 (the size of the entire labeled set), and the size of the negative set $|\mathcal{N}_i|$ to be 4,199. In addition, we use the same hyper-parameters for all of our methods, e.g., hyper-parameter $\alpha = 0.5$ for *HCL*-u, $\beta = 10$ for *HCL*-s and $\alpha = 0.5$ and $\beta = 10$ for *HCL*.

In Figure 1 (a), the y-axis is the performance of methods in terms of F1 score, and the left-hand-side and the right-hand-side of this figure show the performance of four methods for N-MNIST-2v and N-MNIST at noise level=1, respectively. In Figure 1 (b), the x-axis is the level of the noise and the y-axis is the performance of methods in terms of F1 score. By observation, we could find that in Figure 1 (a), *HCL*-s achieves the best performance and DNN remains the similar performance in both settings, while the F1 score of both *HCL*-u and *HCL* drop dramatically in the single view setting. *HCL*-u for two views (i.e. Eq. 4) performs better than *HCL*-u for the single view (i.e. Eq. 3). Our guess is that the goal of *HCL*-u for the single view (i.e., Eq. 3) is to maximize the mutual information between the hidden representation and the original input feature, which results in introducing noise in the hidden representation if the input feature contains a lot of noise (e.g., 100% in current setting). By observation in Figure 1 (b), in the two view setting, the performance of *HCL*-s and *HCL* is slightly influenced by the noise level and their performance does not change too much as the noise level increases. Therefore, we could make a conclusion that when the input data is contaminated by random noise, *HCL*-u for two views (i.e. Eq. 4) has a better performance than *HCL*-u for the single view (i.e. Eq. 3).

^{††}75% means that 75 percent of pixels are contaminated by random noise.

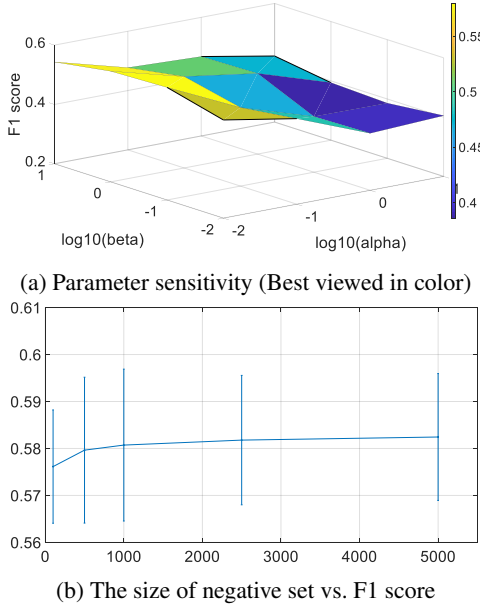


Figure 2: Parameter analysis on XRMB data set

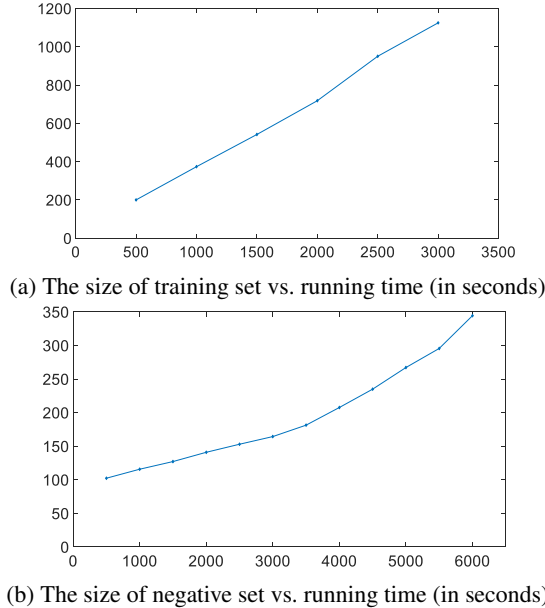


Figure 3: Efficiency analysis on XRMB data set

and HCL -s and HCL are robust enough to handle different levels of noise.

4.5 Parameter Analysis

In this subsection, we analyze the parameter sensitivity of our proposed HCL algorithm on the XRMB data set, including α , β and the size of negative set $|\mathcal{N}_i|$. In all experiments, we use 250 data point as the training set and 49,750 data point as the test set; we set the batch size to be 250, the number of epochs to be 500, the learning rate to

be 0.05 and the optimizer is momentum stochastic gradient descent with Layer-wise Adaptive Rate Scaling scheduler (LARS) [33]. In the first experiment, we fix the size of the negative set $|\mathcal{N}_i|$ to be 4,999, adjust the value of both α and β and record the F1 score of HCL . The results are shown in Figure 2 (a), where the x, y, z axis are the logarithm of α with base 10, the logarithm of β with base 10 and the F1 score. By observation, a large value of β and a small value of α usually leads to a better performance and it achieves the best performance at $\beta = 10$ and $\alpha = 0.01$ or $\log_{10}(\beta) = 1$ and $\log_{10}(\alpha) = -2$. In the second experiment, we fix $\alpha = 0.1$, $\beta = 0.01$, and increase the size of negative set $|\mathcal{N}_i|$ from 100 to 5,000. The experiments are repeated five times and the mean and standard deviation are reported. The results are shown in Figure 2 (b), where the x-axis is the size of the negative set and the y-axis is the F1 score. By observation, we could see that the F1 score of HCL increases as we increase the size of the negative set. Based on the theoretical analysis in Section 3.4 Lemma 3.2, the mutual information between two samples is lower bounded by our proposed weighted unsupervised contrastive loss. As the size of the negative set becomes larger, the lower bound becomes tighter, which is demonstrated by Figure 2 (b). However, as the size of the negative set increases, the computational cost also increases, which will be illustrated in the following subsection.

4.6 Efficiency Analysis

In this subsection, we analyze the efficiency of our proposed HCL algorithm with the different size of the training set and the different size of the negative set $|\mathcal{N}_i|$ on the XRMB data set. In the first experiment, we aim to see how the running time changes when we increase the size of the training set. First, we fix $\alpha = 0.1$, $\beta = 0.01$, the batch size to be 250, the number of epochs to be 500, and the size of negative set $|\mathcal{N}_i|$ to be 999. Then, we set the initial number of training samples to be 500, increase the size of the training set by 500 each time, and record the running time. The results are shown in Figure 3 (a), where the x-axis is the size of the training set or labeled set and the y-axis is the running time. By observation, we could see that the running time is linear to the size of the training set.

In the second experiment, we aim to see how the running time changes when we increase the size of the negative set. We first fix $\alpha = 0.1$, $\beta = 0.01$, the batch size to be 250, the number of epochs to be 500 and the number of training samples to be 250. Then, we set the initial size of negative set $|\mathcal{N}_i|$ to be 500, increase the size of the negative set by 500 each time, and record the running time. The results are shown in Figure 3 (b), where the x-axis is the size of the negative set and the y-axis is the running time. By observation, we could see that the running time is proportional to the square of the size of the negative set. Based on Eq. 4, the negative set $|\mathcal{N}_i|$ is only involved in computing the weighted unsupervised contrastive loss, and for each sample X_i drawn from the entire data set \mathcal{D} , we need to compute the similarity between this sample and the sample drawn from the negative set $|\mathcal{N}_i|$, which gives us $O(n^2)$ time complexity, where n is the size of entire data set \mathcal{D} . Combining the observations in Figure 2 (b) and Figure 3 (b), we could see that there is a trade-off between the computational cost and the performance. The larger the size of the negative set is, the higher performance the algorithm achieves but the higher computational cost it suffers from.

5 CONCLUSION

In this paper, we propose *HCL* - a deep contrastive learning framework for modeling complex heterogeneity. By proposing a weighed unsupervised contrastive loss to model the view heterogeneity, and a weighted supervised contrastive loss to model the label heterogeneity, our proposed framework is capable of handling multiple types of data heterogeneity in the presence of insufficient label information. In addition, we provide theoretical analysis to show that the proposed weighted supervised contrastive loss is the lower bound of the mutual information of two samples from the same class and the weighted unsupervised contrastive loss is the lower bound of the mutual information between the hidden representation of two views of the same sample. The experimental results on real-world data sets demonstrate the effectiveness and efficiency of the proposed framework.

REFERENCES

- [1] S. Akaho. A kernel method for canonical correlation analysis. *CoRR*, abs/0609071, 2006.
- [2] S. Basu, M. Karki, S. Ganguly, R. DiBiano, S. Mukhopadhyay, S. Gayaka, R. Kannan, and R. R. Nemani. Learning sparse feature representations using probabilistic quadtree and deep belief nets. *Neural Process. Lett.*, 45(3):855–867, 2017.
- [3] A. Blum and T. M. Mitchell. Combining labeled and unlabeled data with co-training. In *Proceedings of the Eleventh Annual Conference on Computational Learning Theory, COLT 1998, Madison, Wisconsin, USA, July 24-26, 1998*, pages 92–100. ACM, 1998.
- [4] M. R. Boutell, J. Luo, X. Shen, and C. M. Brown. Learning multi-label scene classification. *Pattern Recognit.*, 37(9):1757–1771, 2004.
- [5] T. Chen, S. Kornblith, M. Norouzi, and G. E. Hinton. A simple framework for contrastive learning of visual representations. In *Proceedings of the 37th International Conference on Machine Learning, ICML 2020, 13-18 July 2020, Virtual Event*, volume 119 of *Proceedings of Machine Learning Research*, pages 1597–1607. PMLR, 2020.
- [6] C. Chuang, J. Robinson, Y. Lin, A. Torralba, and S. Jegelka. Debiased contrastive learning. In *Advances in Neural Information Processing Systems 33: Annual Conference on Neural Information Processing Systems 2020, NeurIPS 2020, December 6-12, 2020, virtual*, 2020.
- [7] J. He and R. Lawrence. A graphbased framework for multi-task multi-view learning. In *Proceedings of the 28th International Conference on Machine Learning, ICML 2011, Bellevue, Washington, USA, June 28 - July 2, 2011*, pages 25–32. Omnipress, 2011.
- [8] Z. Hong, X. Mei, D. V. Prokhorov, and D. Tao. Tracking via robust multi-task multi-view joint sparse representation. In *IEEE International Conference on Computer Vision, ICCV 2013, Sydney, Australia, December 1-8, 2013*, pages 649–656. IEEE Computer Society, 2013.
- [9] S. Huang, W. Gao, and Z. Zhou. Fast multi-instance multi-label learning. In *Proceedings of the Twenty-Eighth AAAI Conference on Artificial Intelligence, July 27 -31, 2014, Québec City, Québec, Canada*, pages 1868–1874. AAAI Press, 2014.
- [10] P. Khosla, P. Teterwak, C. Wang, A. Sarna, Y. Tian, P. Isola, A. Maschinot, C. Liu, and D. Krishnan. Supervised contrastive learning. In *Advances in Neural Information Processing Systems 33: Annual Conference on Neural Information Processing Systems 2020, NeurIPS 2020, December 6-12, 2020, virtual*, 2020.
- [11] S. Kim and E. P. Xing. Tree-guided group lasso for multi-task regression with structured sparsity. In *Proceedings of the 27th International Conference on Machine Learning (ICML-10), June 21-24, 2010, Haifa, Israel*, pages 543–550. Omnipress, 2010.
- [12] G. R. G. Lanckriet, N. Cristianini, P. L. Bartlett, L. E. Ghaoui, and M. I. Jordan. Learning the kernel matrix with semi-definite programming. In *Machine Learning, Proceedings of the Nineteenth International Conference (ICML 2002), University of New South Wales, Sydney, Australia, July 8-12, 2002*, pages 323–330. Morgan Kaufmann, 2002.
- [13] Y. LeCun, L. Bottou, Y. Bengio, and P. Haffner. Gradient-based learning applied to document recognition. *Proceedings of the IEEE*, 86(11):2278–2324, 1998.
- [14] Z. Liu, P. Luo, X. Wang, and X. Tang. Deep learning face attributes in the wild. In *2015 IEEE International Conference on Computer Vision, ICCV 2015, Santiago, Chile, December 7-13, 2015*, pages 3730–3738. IEEE Computer Society, 2015.
- [15] Y. Lu, A. Kumar, S. Zhai, Y. Cheng, T. Javidi, and R. Feris. Fully-adaptive feature sharing in multi-task networks with applications in person attribute classification. In *Proceedings of the IEEE conference on computer vision and pattern recognition*, pages 5334–5343, 2017.
- [16] Y. Luo, D. Tao, C. Xu, D. Li, and C. Xu. Vector-valued multi-view semi-supervised learning for multi-label image classification. In *Proceedings of the Twenty-Seventh AAAI Conference on Artificial Intelligence, July 14-18, 2013, Bellevue, Washington, USA*. AAAI Press, 2013.
- [17] J. Mao, W. Xu, Y. Yang, J. Wang, and A. L. Yuille. Explain images with multimodal recurrent neural networks. *CoRR*, abs/1410.1090, 2014.
- [18] I. Misra, A. Shrivastava, A. Gupta, and M. Hebert. Cross-stitch networks for multi-task learning. In *2016 IEEE Conference on Computer Vision and Pattern Recognition, CVPR 2016, Las Vegas, NV, USA, June 27-30, 2016*, pages 3994–4003. IEEE Computer Society, 2016.
- [19] F. Nie, G. Cai, J. Li, and X. Li. Auto-weighted multi-view learning for image clustering and semi-supervised classification. *IEEE Trans. Image Process.*, 27(3):1501–1511, 2018.
- [20] K. Nigam and R. Ghani. Analyzing the effectiveness and applicability of co-training. In *Proceedings of the 2000 ACM CIKM International Conference on Information and Knowledge Management, McLean, VA, USA, November 6-11, 2000*, pages 86–93. ACM, 2000.
- [21] O. G. R. Pupo, C. Morell, and S. Ventura. Scalable extensions of the relieff algorithm for weighting and selecting features on the multi-label learning context. *Neurocomputing*, 161:168–182, 2015.
- [22] K. Simonyan and A. Zisserman. Very deep convolutional networks for large-scale image recognition. In *3rd International Conference on Learning Representations, ICLR 2015, San Diego, CA, USA, May 7-9, 2015, Conference Track Proceedings*, 2015.
- [23] K. Sohn. Improved deep metric learning with multi-class n-pair loss objective. In *Advances in Neural Information Processing Systems 29: Annual Conference on Neural Information Processing Systems 2016, December 5-10, 2016, Barcelona, Spain*, pages 1849–1857, 2016.
- [24] J. Song and S. Ermon. Multi-label contrastive predictive coding. In *Advances in Neural Information Processing Systems 33: Annual Conference on Neural Information Processing Systems 2020, NeurIPS 2020, December 6-12, 2020, virtual*, 2020.
- [25] Y. Tian, D. Krishnan, and P. Isola. Contrastive multiview coding. In *Computer Vision - ECCV 2020 - 16th European Conference, Glasgow, UK, August 23-28, 2020, Proceedings, Part XI*, volume 12356 of *Lecture Notes in Computer Science*, pages 776–794. Springer, 2020.
- [26] A. van den Oord, Y. Li, and O. Vinyals. Representation learning with contrastive predictive coding. *CoRR*, abs/1807.03748, 2018.
- [27] W. Wang, R. Arora, K. Livescu, and J. A. Bilmes. On deep multi-view representation learning. In *Proceedings of the 32nd International Conference on Machine Learning, ICML 2015, Lille, France, 6-11 July 2015*, volume 37 of *JMLR Workshop and Conference Proceedings*, pages 1083–1092. JMLR.org, 2015.
- [28] J. Westbury. X-ray microbeam speech production database user's handbook: Madison, WI: Waisman Center, University of Wisconsin, 1994.
- [29] C. Xu, D. Tao, and C. Xu. Multi-view intact space learning. *IEEE Trans. Pattern Anal. Mach. Intell.*, 37(12):2531–2544, 2015.
- [30] C. Xu, D. Tao, and C. Xu. Multi-view learning with incomplete views. *IEEE Trans. Image Process.*, 24(12):5812–5825, 2015.
- [31] C. Xu, D. Tao, and C. Xu. Robust extreme multi-label learning. In *Proceedings of the 22nd ACM SIGKDD International Conference on Knowledge Discovery and Data Mining, San Francisco, CA, USA, August 13-17, 2016*, pages 1275–1284. ACM, 2016.
- [32] Y. Yang, Z. Ma, F. Nie, X. Chang, and A. G. Hauptmann. Multi-class active learning by uncertainty sampling with diversity maximization. *Int. J. Comput. Vis.*, 113(2):113–127, 2015.
- [33] Y. You, I. Gitman, and B. Ginsburg. Large batch training of convolutional networks. *arXiv preprint arXiv:1708.03888*, 2017.
- [34] M. Zhang and K. Zhang. Multi-label learning by exploiting label dependency. In *Proceedings of the 16th ACM SIGKDD International Conference on Knowledge Discovery and Data Mining, Washington, DC, USA, July 25-28, 2010*, pages 999–1008. ACM, 2010.
- [35] L. Zheng, Y. Cheng, and J. He. Deep multimodality model for multi-task multi-view learning. In *Proceedings of the 2019 SIAM International Conference on Data Mining, SDM 2019, Calgary, Alberta, Canada, May 2-4, 2019*, pages 10–18. SIAM, 2019.
- [36] D. Zhou and C. J. C. Burges. Spectral clustering and transductive learning with multiple views. In *Machine Learning, Proceedings of the Twenty-Fourth International Conference (ICML 2007), Corvallis, Oregon, USA, June 20-24, 2007*, volume 227 of *ACM International Conference Proceeding Series*, pages 1159–1166. ACM, 2007.
- [37] D. Zhou, L. Zheng, Y. Zhu, J. Li, and J. He. Domain adaptive multi-modality neural attention network for financial forecasting. In *WWW '20: The Web Conference 2020, Taipei, Taiwan, April 20-24, 2020*, pages 2230–2240. ACM / IW3C2, 2020.
- [38] J. Zhou, J. Chen, and J. Ye. Clustered multi-task learning via alternating structure optimization. In *Advances in Neural Information Processing Systems 24: 25th Annual Conference on Neural Information Processing Systems 2011, Proceedings of a meeting held 12-14 December 2011, Granada, Spain*, pages 702–710, 2011.
- [39] Y. Zhu, J. T. Kwok, and Z. Zhou. Multi-label learning with global and local label correlation. *IEEE Trans. Knowl. Data Eng.*, 30(6):1081–1094, 2018.